AEROSPACE REPORT NO.
TOR-2016-01155

AeroCube-6 Dosimeter Data README (v3.0)

March 4, 2016

T. P. O'Brien and J. Bernard Blake
Space Science Applications Laboratory
Physical Sciences Laboratories

Joseph W. Gangestad
Space Superiority Systems Directorate
Space Program Operations

Prepared for:

Space and Missile Systems Center
Air Force Space Command
483 N. Aviation Blvd.
El Segundo, CA 90245-2808

Contract No. FA8802-14-C-0001

Authorized by: Systems Planning, Engineering, and Quality

Abstract

This document serves as a README for the AeroCube-6 level 2 dosimeter data v3.0 release. It includes a brief mission overview, a description of the dosimeters and their operations, and a description of the data files.

Acknowledgments

The authors acknowledge the many Aerospace and government personnel who contributed to the AeroCube-6 mission: D. Hinkley, C. Venturini, J. Avrett, D. Mabry, W. Crain, C. Nguyen, B. Hardy, J. Lee, D. Turner, D. Rowen, C. Coffman, B. Barney, P. Doyle, J. Fuller, D. Pedrino, G. Maul, D. Rumsey, A. Chin, R. Stevens, A Schutte, and D. Arndt.

Contents

Figures

Table

1. AeroCube-6 Mission Overview

The AeroCube-6 (AC6) mission consists of two 0.5U (5x10x10 cm) CubeSats launched on 19 June 2014 into a 620 x 700 km orbit at 98° inclination. The two vehicles are designated AC6-A and AC6-B. Figure 1 shows the stowed and separated configurations of AC6-A and AC6-B. After separation, the two vehicles drift apart due to slight differences in their orbits.

The primary objective of the mission is to demonstrate three new variants of the Aerospace microdosimeter (licensed to Teledyne Microelectronics, Inc.). These additional variants (see next section) enable more energy and species differentiation than is permitted by the baseline dosimeter. The baseline dosimeters have been used to measure dose in lunar and Earth orbit [*Mazur et al.*, 2011; *Mazur et al.,* 2013; *O'Brien et al.*, 2015].

A secondary mission objective is to characterize spatial and temporal structures in low-altitude energetic particles. The scale sizes of these structures in time and space are not only important physical diagnostics of radiation belt loss processes, but they are also important constraints on the use of a space environment measurement on one vehicle to characterize the space environment at another vehicle for anomaly resolution. This kind of remote mapping is a common challenge in satellite anomaly resolution since most satellites do not carry their own environment sensors. Having two satellites is essential to achieving this objective.

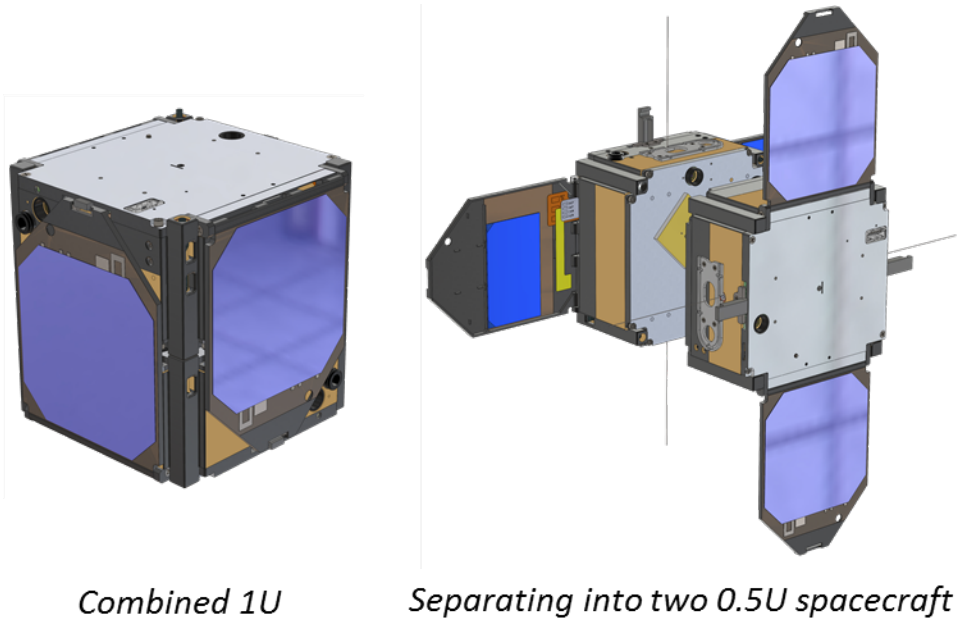

Figure 1. Stowed and separated AC-6 pair. Combined, the two spacecraft conform to the geometry of a single 1U CubeSat. When the satellites' spring-loaded wings open, the reaction force separates the two satellites and they begin to drift apart.

A critical enabling technology for the secondary objective is the use of differential drag, achieved through attitude control. The vehicle attitude is monitored by a Sun sensor and magnetometers. The two CubeSats are approximately Sun-pointing, with a spin rate of about 5 rpm, or a 12-second period. Using magnetic torque rods to adjust the attitude of each satellite, it is possible to cause one vehicle to have a higher drag coefficient than the other. The attitude is allowed to deviate up to ~30° off the nominal Sun pointing without compromising the power needs of the vehicle. This differential drag allows operators to adjust the separation between the two spacecraft (or, more precisely, their separation or closure rate). Figure 2 provides a mission history to date of the AC6 separation distance. The blue line shows the in-track separation between the two spacecraft, and the red line shows the difference in semimajor axis (which affects the rate at which the satellites separate or close). By varying the separation, the two spacecraft can probe different spatial and temporal scales in low-altitude energetic particles.

In order to probe the fine scales, each spacecraft can enter a high-rate mode, changing from nominal 1-Hz dosimeter sample rate to 10-Hz high rate or burst mode. The vehicles can be in this high-rate mode up to about 2/3 of the time and still telemeter all their dosimeter data to the ground.

A tertiary mission objective is to demonstrate autonomous, event-driven radio crosslink between the two satellites. Initially envisioned as a means to have one vehicle trigger a high-rate (burst) mode for the other vehicle, this crosslink was eventually implemented only as a proof-of-concept signaling between the two CubeSats. However, when either vehicle transitions from low-rate to high-rate dosimeter telemetry mode, it does autonomously send a signal to the other CubeSat.

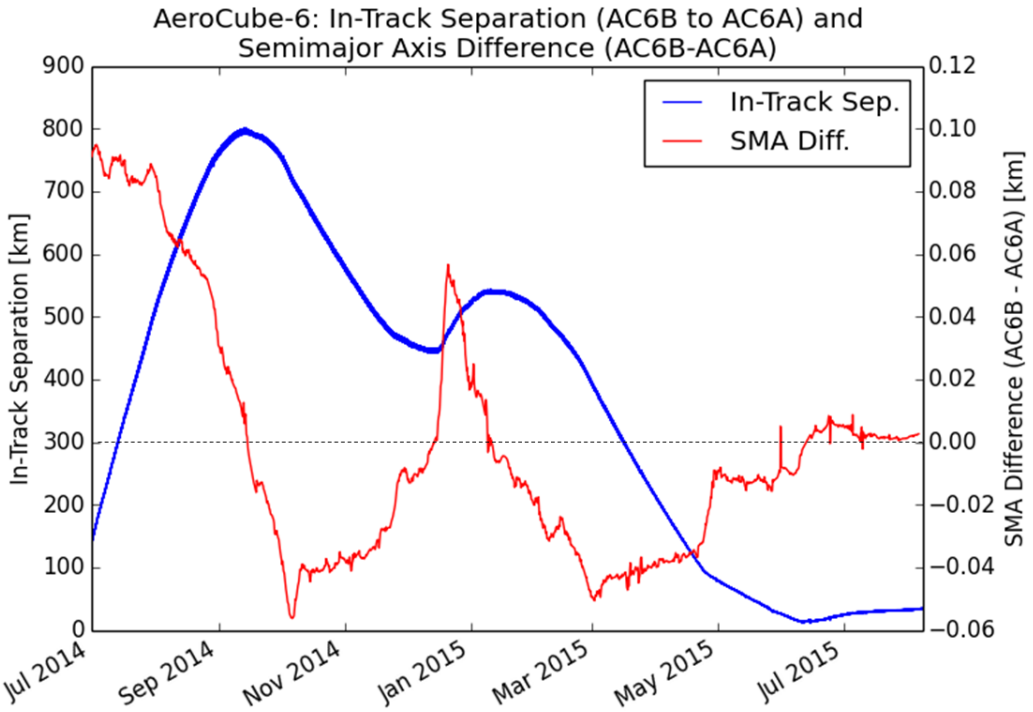

Figure 2. Evolution of AC6 spacecraft separation. The differential drag technique allows operators to adjust the rate of change in the semimajor axis (SMA). The SMA difference between the two vehicles determines the separation/closure rate.

2. AeroCube-6 Dosimeters

Each AeroCube-6 vehicle carries three dosimeters identified as Dos1, Dos2, and Dos3. The dosimeters are mounted on the antisunward side. Figure 3 shows the location of the dosimeters relative to the spacecraft.

Of the 6 dosimeters on AC6, 4 are new variants. On both vehicles, Dos1 and Dos2 are variants that consist of circular silicon detectors 1.8 mm in diameter and 60 μm thick. They are protected from the Sun by a 1.8-μm Al foil that covers their apertures. The electronic system requires a deposit of approximately 30 keV for a count in Dos1, and approximately 250 keV for a count in Dos2. The primary response of Dos1 in the magnetosphere is >35-keV electrons, but it also responds to >235-keV protons (and other particles present in only trace amounts in low Earth orbit). Because the abundance of >35-keV electrons typically exceeds that of >235-keV protons, we treat Dos1 as an electron channel. As for Dos2, because of its higher electronic threshold, it mainly responds to >400-keV protons.

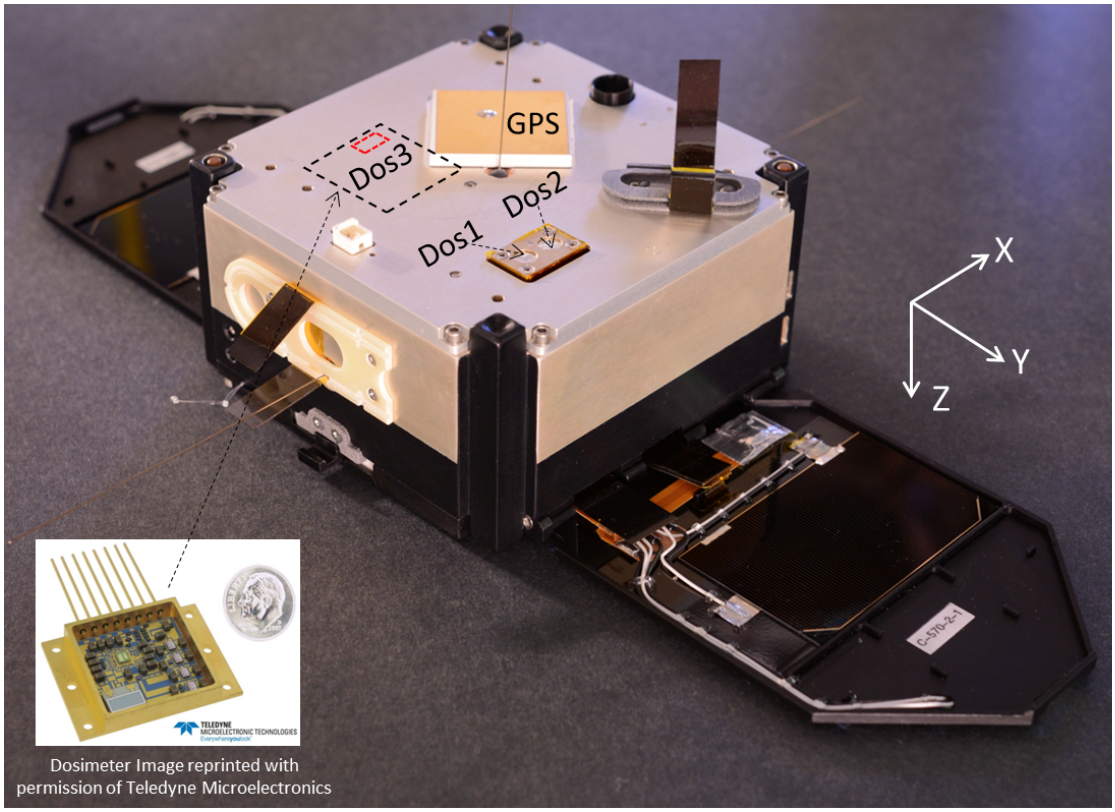

Figure 3. Location of dosimeters. The photograph depicts the location of the three dosimeters on each AC6. Dos3 is internal to the spacecraft, just below the top faceplate. The red rectangle indicates the approximate location of its silicon detector. The GPS antenna is the largest component near the Dos3 field of view. The inset shows what Dos3 would look like with its Kovar lid removed.

However, its electron response has not yet been determined, but the nominal value is >250 keV (i.e., assuming no energy loss in the foil). By using Dos1 and Dos2 together, it is possible to roughly separate >35-keV electron and >400-keV proton populations. The Dos1 sensor counts can be converted to energy deposit using a nominal value of 263.5 μRads per count, but we do not recommend converting Dos2 to dose because of its artificially high electronic threshold.

The Dos3 sensors differ between AC6-A and AC6-B. On AC6-A, Dos3 is the standard or baseline Aerospace-Teledyne microdosimeter [*Mazur et al.*, 2011]. It is behind a minimum of 20 mils Al lid plus a 10-mil Kovar lid thinned to 4 mils over the detector, for a total equivalent of 32 mils Al. An energy deposit of 100 keV is required for a count in the AC6-A Dos3. In the magnetosphere, AC6-A's Dos3 responds to ~1-MeV electrons and >20-MeV protons (and other particles presently only in trace amounts in low Earth orbit). On AC6-B, however, the Dos3 is a variant modified to require 1 MeV energy deposit. This higher threshold filters out most of the electrons. It also partially filters out protons at energies well above the threshold, so that the response is only about 10% for protons with energies of a few hundred MeV. Still, Dos3 on AC6-B measures mainly >20-MeV protons. By using Dos3 on the two vehicles together, it is possible to create separate >1-MeV electron and >20-MeV proton measurements. Based on calibration with a Cobalt-60 gamma ray source, counts from Dos3 on AC6-A can be converted to dose using a nominal value of 14.33 μRads per count. Preliminary proton testing indicates a conversion factor closer to 11 μRads per count, and the difference is still under investigation. Because of its artificially high electronic threshold, we do not recommend converting Dos3 on AC6-B to dose.

Dos1 and Dos2 each have approximately a 60° axially symmetric full angle field of view through the thin foil. The center of this FOV is nominally facing antisunward and in the opposite direction from the vehicle spin axis. There is no barrier separating Dos1 and Dos2, so each also has a narrow secondary FOV through the other's foil. Dos1 and Dos2 also respond to penetrating radiation from all angles. The off-angle response depends on the shielding through which the particles penetrate, and can give rise to spin modulation of the count rate even when the vehicle is spinning exactly around the axis. Dos3 has a rectangular slab geometry (3 mm x 7 mm x 0.25 mm) with a nearly 180° field of view, also centered on the antisunward direction. The nominal 50 mils Al equivalent shielding value applies at nearly normal angles; at nearly grazing incidence angles, the faceplate is 30 mils thicker, and there are obstructions such as the GPS antenna. Because of its rectangular shape, Dos3 also can exhibit spin modulation, even when the vehicle is spinning about the FOV axis. We note that when defining the angle of incidence for particles, we consider particles moving into the detector, thus moving antiparallel to the central axis of the field of view. This is the spacecraft Z axis.

We plan to perform a full Monte Carlo simulation of dosimeter response with the as-flown shielding geometry and electronic thresholds for AC6-A and –B. Until then, all energy, angle, and species response values for the dosimeters must be considered preliminary.

Each dosimeter provides two outputs, a low counter and a medium counter. The low counter represents 0–255 accumulated counts and rolls over at 256. The medium counter accumulates rollovers in the low counter. Thus, the medium and low counters can be combined to produce a total accumulated dose up to $256^2-1 = 65535$ counts before rolling over. In low rate mode, these counters are sampled at 1 Hz. In high rate mode, the medium counters are sampled at 1 Hz, while the low counters are sam-

pled at 10 Hz. We can compute a dose rate by differentiating the dose accumulators with respect to time.

The dose rate calculation requires corrections for single-bit noise and roll-overs. Single-bit noise is relatively easy to detect and correct because the outputs should be monotonically increasing. Roll-overs in the medium are also fairly easy to correct because the medium essentially never rolls over more than once per second. Thus, any large back step in the medium is almost certainly due to a single roll-over. Roll-overs in the low are more difficult to correct because it is possible to encounter multiple roll-overs between 1-second records. Therefore, a smoothed dose that combines the corrected medium and low channels is used to estimate the number of missing roll-overs in the low. This approach accounts for uncertainty in the timing of the medium roll-overs that arises from the single-bit errors and from the fact that, in high-rate mode, the medium is not sampled as often as the low.

Because there is not enough download bandwidth to operate the dosimeters in 10 Hz sample mode at all times, we have defined a region of Earth for low-rate operations. This low-rate zone is within 45° of the magnetic equator with a western boundary at ~130°E geographic longitude and an eastern boundary at ~10°E. We expect highly structured temporal variations (known as microbursts) at magnetic latitudes greater than 45° (i.e., the outer radiation belt), and east of regions of intense lightning. Figure 4 depicts the low-rate zone, the radiation belts, and the Earth's average lightning occurrence rate. We note that we chose to take high-rate data in the longitudes east of Africa because of the intense lightning over Africa and the fact that absent lightning effects, there would normally be no other radiation signatures east of Africa.

During differential drag operations, power constraints can limit dosimeter operations. Also, in August, 2015, AC6-B experienced an unexpected loss of part of its solar array. Thereafter, the maximum dosimeter operational availability is 50%.

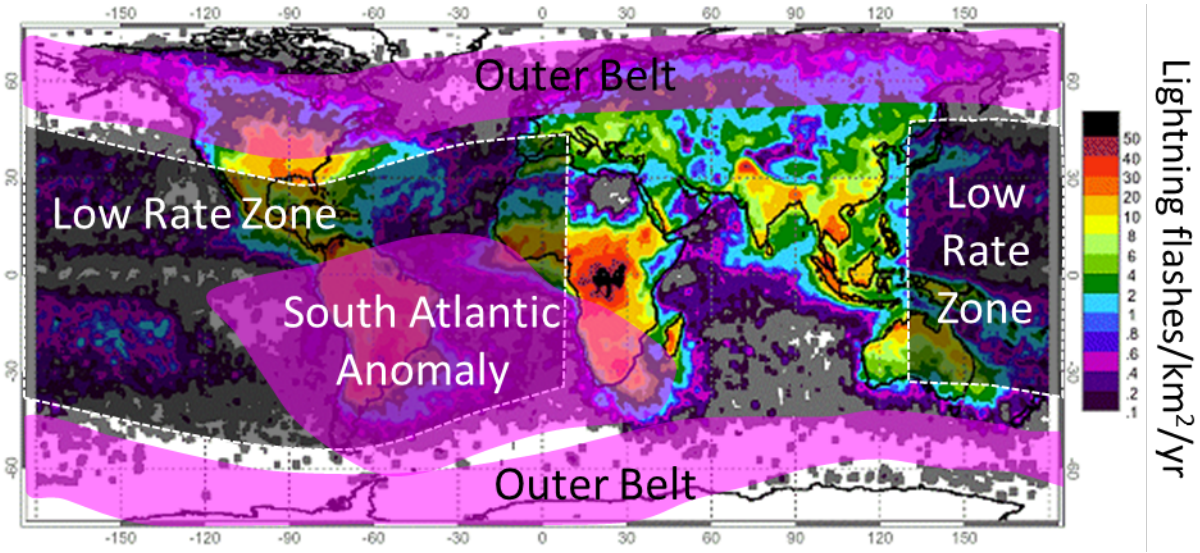

Figure 4. The low rate zone relative to radiation and lightning distributions. Background: Annual lightning climatology (credit: NSSTC Lightning Team at NASA MSFC). Magenta overlay: regions of intense particle radiation. Gray overlay: AC6 low-rate (1 Hz) operations zone. Everywhere else AC6 takes high-rate (10 Hz) data.

There are three main sources of non-geophysical counts (noise) in the dosimeter outputs. The most intense of these occurs near the continental United States, where the transmitter is active for downlink. In addition, any time a vehicle transitions from 1 Hz mode to 10 Hz mode, it activates the transmitter for a crosslink. These transmitter activity times are indicated in the data files by bits set in the "flag" column. Such noise affects all dosimeters. A third noise source has not been diagnosed, but has been attributed to many-day continuous operation of Dos3 on AC6-A. This noise manifests as dosimeter counts usually at high northern latitudes. As we have been unable to identify the specific cause of this noise, we set a flag bit for the entire day in the AC6-A data files. When this flag is set, the entire day of AC6-A Dos3 data is suspect and should only be used with great caution. Starting in Spring 2015, we implemented a periodic turn-off of the AC6-A dosimeters on Sundays to allow the system to recover. This appears to have prevented the noise from returning. The Dos3 noise is present only on certain days from December 2014 to April 2015. The details of these noise flags are given in the next section.

Figure 5 shows a day of AC6-A and AC6-B data as color-coded ground tracks of count rate. AC6-A Dos1 (top, left) shows elevated >35-keV electron fluxes throughout the inner zone (Marker 1, the

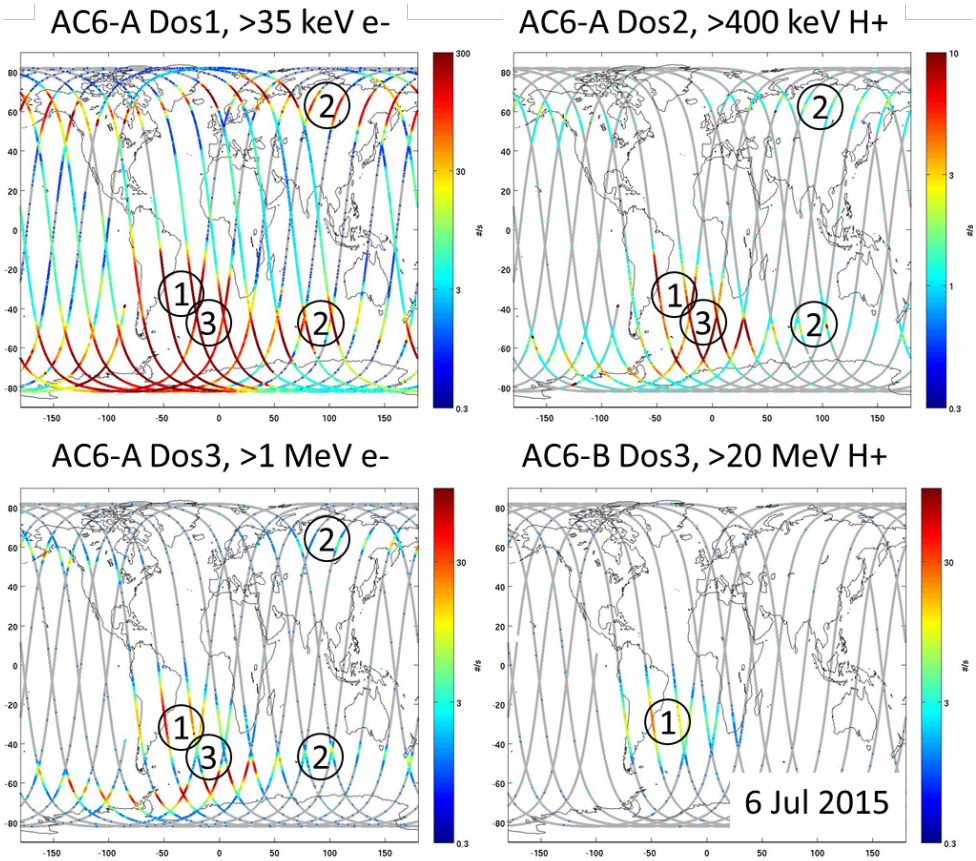

Figure 5. Example dosimeter count rates for 6 July 2015, an active day. The satellite ground tracks for the entire day are color-coded by the count rate for each of the four dosimeter variants. Gray usually indicates zero count rate, but it is also used for rates flagged as noise. Marker 1 indicates the inner zone or South Atlantic Anomaly. Marker 2 indicates the outer zone (high latitude bands). Marker 3 indicates the slot region between the inner and outer zones.

South Atlantic Anomaly), outer zone (Marker 2, high-latitude bands of red), and slot region (Marker 3). AC6-A Dos2 (top, right) shows much weaker signals because of the relatively lesser abundance of >400-keV protons. AC6-A Dos3 (bottom, left) shows the relatively narrow geographic extent of the >1-MeV electrons in the outer zone, as well as >20-MeV protons in the inner zone. AC6-B Dos3 (bottom, right) shows only the South Atlantic Anomaly because there are no >20-MeV protons elsewhere. Comparing AC6-A Dos1 and Dos3, one can see that the lower-energy electrons (Dos1) fill the slot region between the inner zone and the outer zone. This is a common phenomenon observed at high altitude by more sophisticated sensors. It is also noteworthy that Dos1 shows a strong outer zone signature at all longitudes—this is an indicator of relatively stronger loss of ~35-keV electrons into the atmosphere relative to ~1-MeV electrons. Finally, we note that the peak intensity of Dos2 is near the slot region, which suggests Dos2 is not experiencing an electron background of some kind (which would look more like Dos3 on AC6-A); rather, Dos2 is observing a real, if weak, population of >400-keV protons.

3. Data Dictionary

The data to be released are level 2. That is, they include the processed rate product as well as ephemeris and attitude information, and magnetic coordinates.

Table 1 provides the complete data dictionary for the AC6 level 2 data files. Samples from each file type are provided in the appendix. Several general notes and definitions are provided here to assist in the interpretation of the data fields:

- The bad/missing data value for all fields is –1E31 (-10^{31})
- Dose rate is set to missing data after gap of 3 or more seconds.
- Earth Radius, RE, is 6371.2 km. Geodetic coordinates also use the WGS-84 oblate spheroid.
- Flag is a bitmap (bitwise "or" of multiple flags that are powers of 2)
    - 0 – No flags, data are OK
    - 1 – Transmitter on for ground contact. Dosimeters may experience non-physical counts.
    - 2 – Transmitter on for low/high rate transition crosslink. Dosimeters may experience non-physical counts. A 10-second window is flagged either side of the transition from 1 Hz to 10 Hz sampling.
    - 4– Interpolated attitude (30 second or larger gap between inertial fixes). Examine the entire day's Spin-Sun angle to see if the attitude when this flag is set smoothly matches up with attitude when this flag is clear.
    - 8 – Ephemeris from nearest TLE (at least 2 minute gap between ephemeris from smoothed TLE database). This is not necessarily a problem, just a warning.
    - 16 – Dos3 is affected by "northern hemisphere high latitude" noise on this day (AC6-A only). Examine *L* and latitude distribution of dose rate to see which passes and regions are affected.
- GEO – Geographic, Cartesian coordinates. X is through the (0°,0°) latitude longitude point, and Z is through the North geographic pole (Earth's spin axis).
- IGRF – International Geomagnetic Reference Field [*Finaly et al.*, 2010]
- OPQ – Olson-Pfitzer quiet geomagnetic field model [*Olson and Pfitzer*, 1977]
- McIlwain L – McIlwain's magnetic *L* shell parameter [*McIlwain*, 1961]. Also expressed as invariant latitude: $\cos^2\lambda = L^{-1}$.
- L* (Lstar) – Roederer's magnet *L* shell parameter [*Roederer*, 1970]
- K – Kaufmann's modified bounce invariant [*Kaufmann*, 1965]: We adopt the customary definition of *K*: $K = \int_{s_m}^{s_{m'}} [B_m - B(s)]^{1/2} ds$. The limits of integration are the southern and northern mirror points of the particle's bounce motion, *s* is the distance along the magnetic field line, *B(s)* is the magnetic field strength at *s*, and B_m is the mirror point magnetic field strength.
- α (Alpha) – the angle between a particle's momentum and the magnetic field direction.. A locally mirroring particle has $\alpha = 90°$ at the spacecraft.

- α_{eq} (Alpha_Eq) – the angle between a particle's momentum and the magnetic field direction when the particle crosses northward through the weakest point along the magnetic field (the magnetic equator).
- β (beta) – the phase angle of a particle as it gyrates around the local magnetic field. Zero degree particles are normally incident when the dosimeter is facing the Earth (nadir), 90° particles are normally incident when the dosimeter is facing West; 180° particles when facing away from Earth (zenith), and –90° particles when facing East.
- Φ_B (Phi_B) – the longitude of the local magnetic field vector projected into the spacecraft X-Y plane. Zero corresponds to the X axis.
- Ω (Omega) – spin vector, whose length is the spin rate in radians/s.

Table 1. Data Dictionary. An "x" in the 3rd-6th columns indicates which files include each field.

Column	Units	1 Hz Survey	1 Hz Mag Coords	1 Hz Attitude	10 Hz	Description
year		x	x	x	x	
month		x	x	x	x	
day		x	x	x	x	
hour		x	x	x	x	
minute		x	x	x	x	
second		x	x	x	x	
alt	km	x	x	x	x	Geodetic altitude
lat	deg	x	x	x	x	Geodetic latitude
lon	deg	x	x	x	x	Geodetic longitude
X_GEO	RE	x				X-GEO component of location
Y_GEO	RE	x				Y-GEO component of location
Z_GEO	RE	x				Z-GEO component of location
dos1l	counts	x			x	Dos1 low output
dos1m	counts	x			x	Dos1 medium output
dos1rate	#/s	x	x	x	x	Dos1 count rate
dos2l	counts	x			x	Dos2 low output
dos2m	counts	x			x	Dos2 medium output
dos2rate	#/s	x	x	x	x	Dos2 count rate
dos3l	counts	x			x	Dos3 low output
dos3m	counts	x			x	Dos3 medium output
dos3rate	#/s	x	x	x	x	Dos3 count rate
flag		x	x	x	x	Bitmap (see notes)
Sample_Rate	Hz	x				Sample rate, 1 or 10 Hz
Subcom					x	Slot in multiplexed 10 Hz readout, 0 to 9
Lm_IGRF			x			McIlwain L for locally mirroring particle, IGRF magnetic field
Bmag_IGRF	nT		x			Magnitude of IGRF magnetic field at vehicle
MLT_IGRF	hours		x			Solar local time at equatorial crossing of IGRF magnetic field line through vehicle
InvLat_IGRF	deg		x			Invariant latitude (McIlwain L) for locally mirroring particle, IGRF magnetic field
Lm_OPQ		x	x		x	McIlwain L for locally mirroring particle, OPQ magnetic field
Bmag_OPQ	nT	x	x		x	Magnitude of OPQ magnetic field at vehicle
MLT_OPQ	hours	x	x		x	Solar local time at equatorial crossing of OPQ magnetic field line through vehicle
InvLat_OPQ	deg	x	x		x	Invariant latitude (McIlwain L) for locally mirroring particle, OPQ magnetic field

Column	Units	1 Hz Survey	1 Hz Mag Coords	1 Hz Attitude	10 Hz	Description
Loss_Cone_Type		x	x		x	0 - trapped, 1 - drift loss cone, 2 - bounce loss cone, -1 = open/unknown, for locally mirroring particles, OPQ magnetic field
Bx_GEO	nT		x			X-GEO component of local magnetic field, OPQ model
By_GEO	nT		x			Y-GEO component of local magnetic field, OPQ model
Bz_GEO	nT		x			Z-GEO component of local magnetic field, OPQ model
Beq	nT		x			Minimum magnetic field strength on field line through vehicle, OPQ magnetic field
I	RE		x			Integral invariant for locally mirroring particle, OPQ magnetic field
K	$G^{1/2}R_E$		x			Kaufmann invariant for locally mirroring particle, OPQ magnetic field
K_Z	$G^{1/2}R_E$		x		x	Kaufmann invariant for normally incident particle, OPQ magnetic field
Lstar		x	x			Modified third invariant (L*) for locally mirroring particle, OPQ magnetic field
Lstar_Z			x		x	Modified third invariant (L*) for normally incident particle, OPQ magnetic field
hmin	km	x	x			Minum mirror altitude around drift shell for locally mirroring particle, OPQ magnetic field
hmin_Z	km		x		x	Minum mirror altitude around drift shell for normally incident particle, OPQ magnetic field
Loss_Cone_Near	deg		x			Polar angle of near hemisphere loss cone (100 km), OPQ magnetic field
Loss_Cone_Far	deg		x			Polar angle of opposite hemisphere loss cone (100 km), OPQ magnetic field
B100N	nT		x			OPQ magnetic field strength at 100 km altitude, northern hemisphere on field line through vehicle
LAT100N	deg		x			Geodetic latitude at 100 km altitude, northern hemisphere, on OPQ magnetic field line through vehicle
LON100N	deg		x			Geodetic longitude at 100 km altitude, northern hemisphere, on OPQ magnetic field line through vehicle
B100S	nT		x			OPQ magnetic field strength at 100 km altitude, southern hemisphere on field line through vehicle
LAT100S	deg		x			Geodetic latitude at 100 km altitude, southern hemisphere, on OPQ magnetic field line through vehicle
LON100S	deg		x			Geodetic longitude at 100 km altitude, southern hemisphere, on OPQ magnetic field line through vehicle
Alpha	deg	x		x	x	Local pitch angle of normally incident particle, OPQ magnetic field
Alpha_X	deg			x		Local pitch angle of particle moving along spacecraft X axis, OPQ magnetic field
Alpha_Y	deg			x		Local pitch angle of particle moving along spacecraft Y axis, OPQ magnetic field
Alpha_Eq	deg	x		x		Equatorial pitch angle of normally incident particle, OPQ magnetic field
Beta	deg	x		x	x	Gyrophase angle of normally incident particle, OPQ magnetic field

Column	Units	1 Hz Survey	1 Hz Mag Coords	1 Hz Attitude	10 Hz	Description
Beta_X	deg			x		Gyrophase angle of particle moving along spacecraft X axis, OPQ magnetic field
Beta_Y	deg			x		Gyrophase angle of particle moving along spacecraft Y axis, OPQ magnetic field
Phi_B	deg	x		x		Longitude of OPQ magnetic field in sensor coordinates
OmegaX_GEO	rad/s			x		X-GEO component of spin axis
OmegaY_GEO	rad/s			x		Y-GEO component of spin axis
OmegaZ_GEO	rad/s			x		Z-GEO component of spin axis
B_Spin	deg			x		Angle between OPQ magnetic field and spin axis
Spin_Sun	deg			x		Angle between spin axis and sun
Dist_In_Track	km	x			x	In track distance, AC6A - AC6B
Lag_In_Track	s	x			x	In track time separation, AC6A - AC6B
Dist_Cross_Track_Horiz	km	x			x	Horizontal cross-track distance, AC6A - AC6B, Positive is East
Dist_Cross_Track_Vert	km	x			x	Vertical cross-track distance, AC6A - AC6B
Dist_Total	km	x			x	Total separation distance, AC6A - AC6B

4. References

Blake, J. B., and T. P. O'Brien, "Observations of Small Scale Latitudinal Structure in Energetic Electron Precipitation," submitted to *Journal of Geophysical Research*, 2015.

Finlay, C. C., et al. (2010), "International Geomagnetic Reference Field: The eleventh generation," *Geophys. J. Int.,* **183**(3), 1216-1230, doi:10.1111/j.1365-246X.2010.04804.x.

Kaufmann, R. L., (1965), "Conservation of the first and second adiabatic invariants," *J. Geophys. Res.,* **70**, 2181-6.

Mazur, J. E., W. R. Crain, M. D. Looper, D. J. Mabry, J. B. Blake, A. W. Case, M. J. Golightly, J. C. Kasper, and H. E. Spence (2011), "New measurements of total ionizing dose in the lunar environment," *Space Weather,* **9**, S07002, doi:10.1029/2010SW000641.

Mazur, J. E., L. Friesen, A. Lin, D. Mabry, N. Katz, Y. Dotan, J. George, J.B. Blake, M. Looper, M. Redding, T.P. O'Brien, J. Cha, A. Birkitt, P. Carranza, M. Lalic, F. Fuentes, R. Galvan, and M. McNab (2013)," The Relativistic Proton Spectrometer (RPS) for the Radiation Belt Storm Probes Mission," *Space Sci. Rev.* **179**(1-4), 221-261, doi:10.1007/s11214-012-9926-9.

McIlwain, C. E. (1961), "Coordinates for mapping the distribution of magnetically trapped particles," *J. Geophys. Res.,* **66**, 3681-91.

O'Brien, T. P., J. E. Mazur, T. B. Guild, and M. D. Looper (2015), "Using Polar-orbiting Environmental Satellite data to specify the radiation environment up to 1200 km altitude," *Space Weather,* **13**, doi:10.1002/2015SW001166.

Olson, W. P., and K. A. Pfitzer (1977), *Magnetospheric Magnetic Field Modeling, Annual Scientific Report*, Air Force Office of Scientific Research contract F44620-75-C-0033, McDonnell Douglas Astronautics Co., Huntington Beach, CA.

Roederer, J. G., (1970), *Dynamics of Geomagnetically Trapped Radiation*, Springer-Verlag, New York.

Appendix—Sample Data Files

This appendix contains the first few lines from each of the four L2 data files for August 13, 2015 for AC6-A. As there are sometimes more columns than can be formatted on a single page, some of the examples are broken up into multiple pages.

Table A1. Sample 1 Hz Survey File for AC6-A on 13 August 2015

year	month	day	hour	minute	second	alt	lat	lon	X_GEO	Y_GEO	Z_GEO	dos1l
2015	8	13	0	0	0	632.532	-0.74739	154.886	-0.99626	0.46698	-0.01427	221
2015	8	13	0	0	1	632.566	-0.6859	154.873	-0.99618	0.467211	-0.01309	226
2015	8	13	0	0	2	632.608	-0.6244	154.86	-0.99609	0.467441	-0.01192	232
2015	8	13	0	0	3	632.659	-0.56291	154.848	-0.996	0.467672	-0.01074	236
2015	8	13	0	0	4	632.717	-0.50141	154.835	-0.99592	0.467903	-0.00957	240
2015	8	13	0	0	5	632.784	-0.43992	154.822	-0.99583	0.468134	-0.0084	245
2015	8	13	0	0	6	632.778	-0.37842	154.809	-0.99573	0.468359	-0.00722	251
2015	8	13	0	0	7	632.78	-0.31693	154.797	-0.99564	0.468584	-0.00605	0
2015	8	13	0	0	8	632.79	-0.25544	154.784	-0.99554	0.46881	-0.00488	6
2015	8	13	0	0	9	632.808	-0.19394	154.771	-0.99544	0.469035	-0.0037	10
2015	8	13	0	0	10	632.834	-0.13245	154.758	-0.99534	0.46926	-0.00253	15
2015	8	13	0	0	11	632.869	-0.07096	154.745	-0.99524	0.469485	-0.00135	19
2015	8	13	0	0	12	632.912	-0.00947	154.733	-0.99515	0.469711	-0.00018	23
2015	8	13	0	0	13	632.963	0.052023	154.72	-0.99505	0.469936	0.000993	29
2015	8	13	0	0	14	633.022	0.113513	154.707	-0.99495	0.470161	0.002167	34
2015	8	13	0	0	15	633.089	0.175001	154.694	-0.99485	0.470386	0.003341	39
2015	8	13	0	0	16	633.084	0.236489	154.681	-0.99474	0.470606	0.004514	42
2015	8	13	0	0	17	633.086	0.297976	154.669	-0.99463	0.470826	0.005688	46
2015	8	13	0	0	18	633.097	0.359464	154.656	-0.99452	0.471046	0.006862	53
2015	8	13	0	0	19	633.116	0.420952	154.643	-0.99441	0.471265	0.008036	58
2015	8	13	0	0	20	633.143	0.482439	154.63	-0.9943	0.471485	0.00921	64
2015	8	13	0	0	21	633.178	0.543925	154.618	-0.99419	0.471705	0.010383	70
2015	8	13	0	0	22	633.221	0.605411	154.605	-0.99408	0.471924	0.011557	76
2015	8	13	0	0	23	633.273	0.666896	154.592	-0.99397	0.472144	0.012731	82
2015	8	13	0	0	24	633.333	0.72838	154.579	-0.99386	0.472364	0.013905	86
2015	8	13	0	0	25	633.401	0.789862	154.566	-0.99375	0.472583	0.015078	90
2015	8	13	0	0	26	633.396	0.851345	154.554	-0.99363	0.472797	0.016252	94
2015	8	13	0	0	27	633.399	0.912827	154.541	-0.99351	0.473011	0.017426	100
2015	8	13	0	0	28	633.41	0.974309	154.528	-0.99339	0.473225	0.018599	102
2015	8	13	0	0	29	633.43	1.03579	154.515	-0.99327	0.473439	0.019773	107
2015	8	13	0	0	30	633.458	1.09727	154.503	-0.99315	0.473653	0.020946	113
2015	8	13	0	0	31	633.493	1.15875	154.49	-0.99303	0.473867	0.02212	118
2015	8	13	0	0	32	633.538	1.22023	154.477	-0.99291	0.474081	0.023294	123

dos1m	dos1rate	dos2l	dos2m	dos2rate	dos3l	dos3m	dos3rate	flag	Sample_Ra	Lm_OPQ	Bmag_OPQ	MLT_OPQ
67	-1.00E+31	93	208	-1.00E+31	187	66	-1.00E+31	0	1	1.06537	27730.9	10.4225
67	4.99998	93	208	0	187	66	0	0	1	1.06505	27715.4	10.4214
67	6.00003	93	208	0	187	66	0	0	1	1.06474	27699.8	10.4203
67	3.99998	93	208	0	187	66	0	0	1	1.06442	27684.2	10.4192
67	4.00002	93	208	0	187	66	0	0	1	1.0641	27668.5	10.4181
67	4.99998	93	208	0	187	66	0	0	1	1.06378	27652.9	10.4171
67	6.00003	93	208	0	187	66	0	0	1	1.06344	27638.2	10.416
68	4.99998	93	208	0	187	66	0	0	1	1.06309	27623.5	10.4149
68	6.00003	93	208	0	187	66	0	0	1	1.06266	27608.8	10.4138
68	3.99998	93	208	0	187	66	0	0	1	1.06228	27594.1	10.4127
68	5.00003	93	208	0	187	66	0	0	1	1.06199	27579.3	10.4116
68	3.99998	93	208	0	187	66	0	0	1	1.06169	27564.6	10.4105
68	4.00002	93	208	0	187	66	0	0	1	1.0614	27549.8	10.4094
68	5.99997	93	208	0	187	66	0	0	1	1.06111	27534.9	10.4083
68	4.99998	93	208	0	187	66	0	0	1	1.06081	27520.1	10.4072
68	5.00003	93	208	0	187	66	0	0	1	1.06051	27505.3	10.4061
68	2.99999	93	208	0	187	66	0	0	1	1.06018	27491.4	10.4051
68	4.00002	93	208	0	187	66	0	0	1	1.05981	27477.5	10.404
68	6.99997	93	208	0	187	66	0	0	1	1.05942	27463.6	10.4029
68	5.00003	93	208	0	187	66	0	0	1	1.05915	27449.6	10.4018
68	5.99997	93	208	0	187	66	0	0	1	1.05888	27435.7	10.4007
68	6.00003	93	208	0	187	66	0	0	1	1.0586	27421.7	10.3996
68	5.99997	93	208	0	187	66	0	0	1	1.05833	27407.7	10.3985
68	6.00003	93	208	0	187	66	0	0	1	1.05806	27393.7	10.3974
68	3.99998	93	208	0	187	66	0	0	1	1.05779	27379.7	10.3963
68	4.00002	93	208	0	187	66	0	0	1	1.0575	27365.7	10.3953
68	3.99998	93	208	0	187	66	0	0	1	1.05717	27352.6	10.3942
68	5.99997	93	208	0	187	66	0	0	1	1.05678	27339.6	10.3931
68	2.00001	93	208	0	187	66	0	0	1	1.05653	27326.5	10.392
68	4.99998	93	208	0	187	66	0	0	1	1.05628	27313.3	10.3909
68	6.00003	93	208	0	187	66	0	0	1	1.05603	27300.2	10.3898
68	4.99998	93	208	0	187	66	0	0	1	1.05578	27287.1	10.3888
68	5.00003	93	208	0	187	66	0	0	1	1.05554	27273.9	10.3877

InvLat_OP(	Loss_Cone	Lstar	hmin	Alpha	Alpha_Eq	Beta	Phi_B	Dist_In_Tra	Lag_In_Tra	Dist_Cross_	Dist_Cross_	Dist_Total
-14.3422	1	-1.00E+31	-579.523	56.5973	52.0397	29.6492	-146.48	36.7931	4.87152	-0.03338	0.116619	36.8791
-14.3086	1	-1.00E+31	-577.132	56.5983	52.0963	28.5279	-179.988	36.7935	4.87158	-0.03325	0.116834	36.8794
-14.275	1	-1.00E+31	-574.729	57.1272	52.5997	27.4845	146.555	36.7938	4.87165	-0.03312	0.117049	36.8797
-14.2414	1	-1.00E+31	-572.312	58.0616	53.4444	26.8535	113.331	36.7941	4.87171	-0.033	0.117264	36.8801
-14.2076	1	-1.00E+31	-569.881	59.1481	54.4132	26.8182	80.4278	36.7945	4.87177	-0.03287	0.117479	36.8804
-14.1735	1	-1.00E+31	-567.43	60.0907	55.2577	27.3619	47.8163	36.7948	4.87184	-0.03274	0.117694	36.8807
-14.1373	1	-1.00E+31	-565.058	60.6456	55.7784	28.2923	15.3878	36.7952	4.87191	-0.03261	0.117909	36.8811
-14.0993	1	-1.00E+31	-562.644	60.6921	55.8782	29.309	-17.0055	36.7955	4.87198	-0.03248	0.118125	36.8814
-14.0531	1	-1.00E+31	-560.083	60.2664	55.5853	30.0894	-49.5143	36.7959	4.87205	-0.03236	0.118341	36.8818
-14.013	1	-1.00E+31	-557.603	59.5523	55.0469	30.3766	-82.2651	36.7963	4.87213	-0.03223	0.118557	36.8821
-13.9809	1	-1.00E+31	-555.237	58.8283	54.4934	30.0584	-115.322	36.7967	4.8722	-0.0321	0.118772	36.8825
-13.9489	1	-1.00E+31	-552.86	57.6545	53.5485	29.6713	-148.109	36.7971	4.87227	-0.03197	0.118988	36.8828
-13.9169	1	-1.00E+31	-550.47	57.6677	53.6145	28.4813	178.387	36.7975	4.87234	-0.03184	0.119204	36.8832
-13.8849	1	-1.00E+31	-548.065	58.2455	54.1653	27.3901	144.943	36.7978	4.87241	-0.03171	0.119419	36.8836
-13.8525	1	-1.00E+31	-545.641	59.2497	55.0796	26.7479	111.746	36.7982	4.87249	-0.03158	0.119635	36.8839
-13.8195	1	-1.00E+31	-543.192	60.4044	56.1176	26.7404	78.8797	36.7986	4.87256	-0.03145	0.119851	36.8843
-13.7836	1	-1.00E+31	-540.805	61.3928	57.0102	27.3413	46.3075	36.799	4.87263	-0.03132	0.120068	36.8846
-13.7425	1	-1.00E+31	-538.308	61.9574	57.5445	28.3411	13.9154	36.7994	4.8727	-0.03119	0.120285	36.885
-13.6995	1	-1.00E+31	-535.761	61.9751	57.6202	29.4195	-18.4474	36.7997	4.87277	-0.03106	0.120502	36.8853
-13.6691	1	-1.00E+31	-533.424	61.4912	57.2726	30.2358	-50.9325	36.8001	4.87284	-0.03093	0.120719	36.8856
-13.6388	1	-1.00E+31	-531.076	60.7072	56.6655	30.5224	-83.6672	36.8005	4.87291	-0.03079	0.120936	36.886
-13.6086	1	-1.00E+31	-528.716	59.9239	56.0514	30.1666	-116.716	36.8009	4.87299	-0.03066	0.121153	36.8863
-13.5783	1	-1.00E+31	-526.34	59.4496	55.6975	29.2614	-150.044	36.8012	4.87306	-0.03053	0.12137	36.8867
-13.5478	1	-1.00E+31	-523.947	59.0501	55.4053	27.838	176.503	36.8016	4.87313	-0.0304	0.121587	36.887
-13.5168	1	-1.00E+31	-521.528	59.6678	55.9959	26.8357	143.121	36.802	4.8732	-0.03027	0.121804	36.8874
-13.4846	1	-1.00E+31	-519.072	60.6718	56.9196	26.2868	109.978	36.8024	4.87327	-0.03014	0.122021	36.8877
-13.4473	1	-1.00E+31	-516.628	61.788	57.9357	26.3478	77.1368	36.8026	4.87332	-0.03001	0.122238	36.888
-13.403	1	-1.00E+31	-514.022	62.713	58.784	26.974	44.5568	36.8028	4.87337	-0.02988	0.122456	36.8882
-13.3743	1	-1.00E+31	-511.716	63.2094	59.2657	27.9512	12.1275	36.803	4.87342	-0.02974	0.122673	36.8885
-13.3458	1	-1.00E+31	-509.4	63.1751	59.2963	28.967	-20.2911	36.8032	4.87347	-0.02961	0.12289	36.8888
-13.3174	1	-1.00E+31	-507.072	62.6721	58.9254	29.6995	-52.8362	36.8035	4.87352	-0.02948	0.123107	36.889
-13.2891	1	-1.00E+31	-504.73	61.9093	58.3257	29.9064	-85.6198	36.8037	4.87358	-0.02935	0.123324	36.8893
-13.2605	1	-1.00E+31	-502.37	61.1823	57.7498	29.5024	-118.691	36.8039	4.87363	-0.02922	0.123541	36.8895

Table A2. Sample 1 Hz Magnetic Coordinates File for AC6-A on 13 August 2015

year	month	day	hour	minute	second	alt	lat	lon	dos1rate	dos2rate	dos3rate	flag
2015	8	13	0	0	0	632.532	-0.74739	154.886	-1.00E+31	-1.00E+31	-1.00E+31	0
2015	8	13	0	0	1	632.566	-0.6859	154.873	4.99998	0	0	0
2015	8	13	0	0	2	632.608	-0.6244	154.86	6.00003	0	0	0
2015	8	13	0	0	3	632.659	-0.56291	154.848	3.99998	0	0	0
2015	8	13	0	0	4	632.717	-0.50141	154.835	4.00002	0	0	0
2015	8	13	0	0	5	632.784	-0.43992	154.822	4.99998	0	0	0
2015	8	13	0	0	6	632.778	-0.37842	154.809	6.00003	0	0	0
2015	8	13	0	0	7	632.78	-0.31693	154.797	4.99998	0	0	0
2015	8	13	0	0	8	632.79	-0.25544	154.784	6.00003	0	0	0
2015	8	13	0	0	9	632.808	-0.19394	154.771	3.99998	0	0	0
2015	8	13	0	0	10	632.834	-0.13245	154.758	5.00003	0	0	0
2015	8	13	0	0	11	632.869	-0.07096	154.745	3.99998	0	0	0
2015	8	13	0	0	12	632.912	-0.00947	154.733	4.00002	0	0	0
2015	8	13	0	0	13	632.963	0.052023	154.72	5.99997	0	0	0
2015	8	13	0	0	14	633.022	0.113513	154.707	4.99998	0	0	0
2015	8	13	0	0	15	633.089	0.175001	154.694	5.00003	0	0	0
2015	8	13	0	0	16	633.084	0.236489	154.681	2.99999	0	0	0
2015	8	13	0	0	17	633.086	0.297976	154.669	4.00002	0	0	0
2015	8	13	0	0	18	633.097	0.359464	154.656	6.99997	0	0	0
2015	8	13	0	0	19	633.116	0.420952	154.643	5.00003	0	0	0
2015	8	13	0	0	20	633.143	0.482439	154.63	5.99997	0	0	0
2015	8	13	0	0	21	633.178	0.543925	154.618	6.00003	0	0	0
2015	8	13	0	0	22	633.221	0.605411	154.605	5.99997	0	0	0
2015	8	13	0	0	23	633.273	0.666896	154.592	6.00003	0	0	0
2015	8	13	0	0	24	633.333	0.72838	154.579	3.99998	0	0	0
2015	8	13	0	0	25	633.401	0.789862	154.566	4.00002	0	0	0
2015	8	13	0	0	26	633.396	0.851345	154.554	3.99998	0	0	0
2015	8	13	0	0	27	633.399	0.912827	154.541	5.99997	0	0	0
2015	8	13	0	0	28	633.41	0.974309	154.528	2.00001	0	0	0
2015	8	13	0	0	29	633.43	1.03579	154.515	4.99998	0	0	0
2015	8	13	0	0	30	633.458	1.09727	154.503	6.00003	0	0	0
2015	8	13	0	0	31	633.493	1.15875	154.49	4.99998	0	0	0
2015	8	13	0	0	32	633.538	1.22023	154.477	5.00003	0	0	0

Lm_IGRF	Bmag_IGR	MLT_IGRF	InvLat_IGR	Lm_OPQ	Bmag_OPQ	MLT_OPQ	InvLat_OPQ	Loss_Cone	Bx_GEO	By_GEO	Bz_GEO	Beq
1.06537	27730.9	10.4225	-14.3422	1.06537	27730.9	10.4225	-14.3422	1	-8376.94	783.85	26423.8	24734.9
1.06505	27715.4	10.4214	-14.3086	1.06505	27715.4	10.4214	-14.3086	1	-8294.99	753.436	26434.2	24758.6
1.06474	27699.8	10.4203	-14.275	1.06474	27699.8	10.4203	-14.275	1	-8213.02	722.993	26444.3	24782
1.06442	27684.2	10.4192	-14.2414	1.06442	27684.2	10.4192	-14.2414	1	-8131.04	692.523	26454.1	24805.1
1.0641	27668.5	10.4181	-14.2076	1.0641	27668.5	10.4181	-14.2076	1	-8049.04	662.025	26463.6	24828
1.06378	27652.9	10.4171	-14.1735	1.06378	27652.9	10.4171	-14.1735	1	-7967.03	631.501	26472.8	24850.7
1.06344	27638.2	10.416	-14.1373	1.06344	27638.2	10.416	-14.1373	1	-7885.27	600.949	26482.7	24873.9
1.06309	27623.5	10.4149	-14.0993	1.06309	27623.5	10.4149	-14.0993	1	-7803.49	570.368	26492.3	24896.9
1.06266	27608.8	10.4138	-14.0531	1.06266	27608.8	10.4138	-14.0531	1	-7721.69	539.76	26501.5	24919.7
1.06228	27594.1	10.4127	-14.013	1.06228	27594.1	10.4127	-14.013	1	-7639.87	509.124	26510.5	24942.2
1.06199	27579.3	10.4116	-13.9809	1.06199	27579.3	10.4116	-13.9809	1	-7558.04	478.463	26519.2	24964.5
1.06169	27564.6	10.4105	-13.9489	1.06169	27564.6	10.4105	-13.9489	1	-7476.2	447.776	26527.5	24986.6
1.0614	27549.8	10.4094	-13.9169	1.0614	27549.8	10.4094	-13.9169	1	-7394.35	417.064	26535.6	25008.3
1.06111	27534.9	10.4083	-13.8849	1.06111	27534.9	10.4083	-13.8849	1	-7312.49	386.327	26543.4	25029.9
1.06081	27520.1	10.4072	-13.8525	1.06081	27520.1	10.4072	-13.8525	1	-7230.61	355.567	26550.9	25051.2
1.06051	27505.3	10.4061	-13.8195	1.06051	27505.3	10.4061	-13.8195	1	-7148.74	324.783	26558	25072.2
1.06018	27491.4	10.4051	-13.7836	1.06018	27491.4	10.4051	-13.7836	1	-7067.09	293.964	26565.9	25093.9
1.05981	27477.5	10.404	-13.7425	1.05981	27477.5	10.404	-13.7425	1	-6985.43	263.12	26573.4	25115.3
1.05942	27463.6	10.4029	-13.6995	1.05942	27463.6	10.4029	-13.6995	1	-6903.75	232.252	26580.7	25136.5
1.05915	27449.6	10.4018	-13.6691	1.05915	27449.6	10.4018	-13.6691	1	-6822.08	201.36	26587.6	25157.4
1.05888	27435.7	10.4007	-13.6388	1.05888	27435.7	10.4007	-13.6388	1	-6740.39	170.445	26594.3	25178.1
1.0586	27421.7	10.3996	-13.6086	1.0586	27421.7	10.3996	-13.6086	1	-6658.7	139.508	26600.6	25198.5
1.05833	27407.7	10.3985	-13.5783	1.05833	27407.7	10.3985	-13.5783	1	-6577	108.55	26606.7	25218.6
1.05806	27393.7	10.3974	-13.5478	1.05806	27393.7	10.3974	-13.5478	1	-6495.3	77.5703	26612.4	25238.5
1.05779	27379.7	10.3963	-13.5168	1.05779	27379.7	10.3963	-13.5168	1	-6413.6	46.5701	26617.9	25258.1
1.0575	27365.7	10.3953	-13.4846	1.0575	27365.7	10.3953	-13.4846	1	-6331.91	15.5505	26623.1	25277.5
1.05717	27352.6	10.3942	-13.4473	1.05717	27352.6	10.3942	-13.4473	1	-6250.41	-15.5141	26628.9	25297.4
1.05678	27339.6	10.3931	-13.403	1.05678	27339.6	10.3931	-13.403	1	-6168.92	-46.6001	26634.4	25317.2
1.05653	27326.5	10.392	-13.3743	1.05653	27326.5	10.392	-13.3743	1	-6087.42	-77.7066	26639.7	25336.7
1.05628	27313.3	10.3909	-13.3458	1.05628	27313.3	10.3909	-13.3458	1	-6005.92	-108.834	26644.6	25356
1.05603	27300.2	10.3898	-13.3174	1.05603	27300.2	10.3898	-13.3174	1	-5924.42	-139.98	26649.3	25375
1.05578	27287.1	10.3888	-13.2891	1.05578	27287.1	10.3888	-13.2891	1	-5842.92	-171.145	26653.6	25393.7
1.05554	27273.9	10.3877	-13.2605	1.05554	27273.9	10.3877	-13.2605	1	-5761.42	-202.329	26657.7	25412.2

I	K	K_Z	Lstar	Lstar_Z	hmin	hmin_Z	Loss_Cone	Loss_Cone	B100N	LAT100N	LON100N	B100S
0.090562	0.04769	-1.00E+31	-1.00E+31	-1.00E+31	-579.523	-1.00E+31	56.068	61.9683	35591.8	24.6966	156.677	40283
0.089406	0.047068	-1.00E+31	-1.00E+31	-1.00E+31	-577.132	-1.00E+31	56.0559	61.948	35585.3	24.671	156.655	40271.9
0.088253	0.046448	0.227058	-1.00E+31	-1.00E+31	-574.729	-1.00E+31	56.044	61.9281	35578.4	24.6453	156.633	40260.4
0.087101	0.045829	0.213852	-1.00E+31	-1.00E+31	-572.312	-1.00E+31	56.0326	61.9088	35571.2	24.6196	156.611	40248.6
0.085946	0.045209	0.199472	-1.00E+31	-1.00E+31	-569.881	-1.00E+31	56.0214	61.8661	35579.5	24.6046	156.589	40236.4
0.084786	0.044586	0.187575	-1.00E+31	-1.00E+31	-567.43	-1.00E+31	56.0107	61.8478	35571.5	24.5788	156.567	40223.8
0.08361	0.043956	0.180533	-1.00E+31	-1.00E+31	-565.058	-1.00E+31	56.0002	61.8301	35564.4	24.553	156.545	40212.4
0.0824	0.043308	0.17923	-1.00E+31	-1.00E+31	-562.644	-1.00E+31	55.9901	61.8129	35556.9	24.5272	156.523	40200.5
0.081017	0.042569	0.18319	-1.00E+31	-1.00E+31	-560.083	-1.00E+31	55.9803	61.7961	35549.1	24.5013	156.501	40188.4
0.079766	0.041901	0.190622	-1.00E+31	-1.00E+31	-557.603	-1.00E+31	55.9709	61.7799	35540.9	24.4754	156.479	40175.8
0.078684	0.041322	0.198504	-1.00E+31	-1.00E+31	-555.237	-1.00E+31	55.9619	61.7406	35548.1	24.4601	156.457	40162.9
0.077605	0.040744	0.212535	-1.00E+31	-1.00E+31	-552.86	-1.00E+31	55.9531	61.7254	35539.2	24.4341	156.436	40149.7
0.076528	0.040168	0.211566	-1.00E+31	-1.00E+31	-550.47	-1.00E+31	55.9448	61.7107	35529.9	24.4081	156.414	40136.1
0.07545	0.039591	0.203375	-1.00E+31	-1.00E+31	-548.065	-1.00E+31	55.9141	61.673	35536	24.3928	156.392	40143.6
0.074366	0.039012	0.190318	-1.00E+31	-1.00E+31	-545.641	-1.00E+31	55.9064	61.6593	35526	24.3667	156.37	40129.2
0.073271	0.038428	0.176297	-1.00E+31	-1.00E+31	-543.192	-1.00E+31	55.8991	61.6461	35515.7	24.3406	156.348	40114.5
0.072147	0.037829	0.164895	-1.00E+31	-1.00E+31	-540.805	-1.00E+31	55.8921	61.6101	35521.8	24.3251	156.327	40100.8
0.070917	0.037174	0.158356	-1.00E+31	-1.00E+31	-538.308	-1.00E+31	55.8855	61.598	35512	24.299	156.305	40086.8
0.069653	0.036502	0.157469	-1.00E+31	-1.00E+31	-535.761	-1.00E+31	55.8792	61.5864	35501.8	24.2728	156.283	40072.5
0.068644	0.035964	0.161727	-1.00E+31	-1.00E+31	-533.424	-1.00E+31	55.8733	61.552	35506.8	24.2572	156.262	40057.8
0.067639	0.035429	0.169352	-1.00E+31	-1.00E+31	-531.076	-1.00E+31	55.8452	61.5414	35495.9	24.231	156.24	40064
0.066636	0.034895	0.177342	-1.00E+31	-1.00E+31	-528.716	-1.00E+31	55.84	61.5081	35500.2	24.2154	156.218	40048.6
0.065634	0.034361	0.182089	-1.00E+31	-1.00E+31	-526.34	-1.00E+31	55.8352	61.4985	35488.6	24.189	156.197	40032.7
0.064628	0.033826	0.186087	-1.00E+31	-1.00E+31	-523.947	-1.00E+31	55.8307	61.4663	35492.1	24.1734	156.175	40016.6
0.063613	0.033286	0.178161	-1.00E+31	-1.00E+31	-521.528	-1.00E+31	55.8042	61.4577	35479.7	24.147	156.154	40021.2
0.062575	0.032734	0.166276	-1.00E+31	-1.00E+31	-519.072	-1.00E+31	55.8004	61.4266	35482.5	24.1313	156.132	40004.3
0.061466	0.032146	0.153906	-1.00E+31	-1.00E+31	-516.628	-1.00E+31	55.797	61.4191	35470.7	24.1048	156.111	39988.5
0.060219	0.031487	0.144125	-1.00E+31	-1.00E+31	-514.022	-1.00E+31	55.7939	61.3891	35473.9	24.089	156.089	39972.3
0.059283	0.03099	0.13879	-1.00E+31	-1.00E+31	-511.716	-1.00E+31	55.7689	61.3825	35461.4	24.0625	156.068	39976.8
0.058352	0.030496	0.138479	-1.00E+31	-1.00E+31	-509.4	-1.00E+31	55.7665	61.3536	35463.9	24.0467	156.046	39959.9
0.057424	0.030004	0.142612	-1.00E+31	-1.00E+31	-507.072	-1.00E+31	55.7645	61.3253	35466	24.0308	156.025	39942.6
0.056497	0.029513	0.149468	-1.00E+31	-1.00E+31	-504.73	-1.00E+31	55.7407	61.3202	35452.4	24.0043	156.004	39946
0.055568	0.02902	0.156279	-1.00E+31	-1.00E+31	-502.37	-1.00E+31	55.7394	61.2929	35453.8	23.9883	155.982	39927.9

LAT100S	LON100S
-10.3948	153.731
-10.3691	153.716
-10.3433	153.7
-10.3176	153.685
-10.2919	153.67
-10.2662	153.654
-10.2405	153.639
-10.2148	153.624
-10.1891	153.608
-10.1634	153.593
-10.1378	153.578
-10.1122	153.563
-10.0865	153.547
-10.0714	153.531
-10.0458	153.516
-10.0203	153.5
-9.99468	153.485
-9.96912	153.47
-9.94357	153.455
-9.91803	153.44
-9.90304	153.423
-9.87752	153.408
-9.85202	153.393
-9.82652	153.378
-9.81158	153.361
-9.78611	153.346
-9.76065	153.331
-9.73521	153.316
-9.72032	153.3
-9.69489	153.285
-9.66948	153.27
-9.65463	153.253
-9.62923	153.238

Table A3. Sample 1 Hz Attitude File for AC6-A on 13 August 2015

year	month	day	hour	minute	second	alt	lat	lon	dos1rate	dos2rate	dos3rate	flag
2015	8	13	0	0	0	632.532	-0.74739	154.886	-1.00E+31	-1.00E+31	-1.00E+31	0
2015	8	13	0	0	1	632.566	-0.6859	154.873	4.99998	0	0	0
2015	8	13	0	0	2	632.608	-0.6244	154.86	6.00003	0	0	0
2015	8	13	0	0	3	632.659	-0.56291	154.848	3.99998	0	0	0
2015	8	13	0	0	4	632.717	-0.50141	154.835	4.00002	0	0	0
2015	8	13	0	0	5	632.784	-0.43992	154.822	4.99998	0	0	0
2015	8	13	0	0	6	632.778	-0.37842	154.809	6.00003	0	0	0
2015	8	13	0	0	7	632.78	-0.31693	154.797	4.99998	0	0	0
2015	8	13	0	0	8	632.79	-0.25544	154.784	6.00003	0	0	0
2015	8	13	0	0	9	632.808	-0.19394	154.771	3.99998	0	0	0
2015	8	13	0	0	10	632.834	-0.13245	154.758	5.00003	0	0	0
2015	8	13	0	0	11	632.869	-0.07096	154.745	3.99998	0	0	0
2015	8	13	0	0	12	632.912	-0.00947	154.733	4.00002	0	0	0
2015	8	13	0	0	13	632.963	0.052023	154.72	5.99997	0	0	0
2015	8	13	0	0	14	633.022	0.113513	154.707	4.99998	0	0	0
2015	8	13	0	0	15	633.089	0.175001	154.694	5.00003	0	0	0
2015	8	13	0	0	16	633.084	0.236489	154.681	2.99999	0	0	0
2015	8	13	0	0	17	633.086	0.297976	154.669	4.00002	0	0	0
2015	8	13	0	0	18	633.097	0.359464	154.656	6.99997	0	0	0
2015	8	13	0	0	19	633.116	0.420952	154.643	5.00003	0	0	0
2015	8	13	0	0	20	633.143	0.482439	154.63	5.99997	0	0	0
2015	8	13	0	0	21	633.178	0.543925	154.618	6.00003	0	0	0
2015	8	13	0	0	22	633.221	0.605411	154.605	5.99997	0	0	0
2015	8	13	0	0	23	633.273	0.666896	154.592	6.00003	0	0	0
2015	8	13	0	0	24	633.333	0.72838	154.579	3.99998	0	0	0
2015	8	13	0	0	25	633.401	0.789862	154.566	4.00002	0	0	0
2015	8	13	0	0	26	633.396	0.851345	154.554	3.99998	0	0	0
2015	8	13	0	0	27	633.399	0.912827	154.541	5.99997	0	0	0
2015	8	13	0	0	28	633.41	0.974309	154.528	2.00001	0	0	0
2015	8	13	0	0	29	633.43	1.03579	154.515	4.99998	0	0	0
2015	8	13	0	0	30	633.458	1.09727	154.503	6.00003	0	0	0
2015	8	13	0	0	31	633.493	1.15875	154.49	4.99998	0	0	0
2015	8	13	0	0	32	633.538	1.22023	154.477	5.00003	0	0	0

Alpha	Alpha_X	Alpha_Y	Alpha_Eq	Beta	Beta_X	Beta_Y	Phi_B	OmegaX_G	OmegaY_G	OmegaZ_G	B_Spin	Spin_Sun
56.5973	134.106	117.452	52.0397	29.6492	-20.6198	99.6148	-146.48	-0.55468	-0.01774	0.142933	58.0509	0.679243
56.5983	146.598	90.0104	52.0963	28.5279	28.5052	118.521	-179.988	-0.55468	-0.0177	0.142933	58.2152	0.679232
57.1272	134.492	62.4265	52.5997	27.4845	78.0724	137.208	146.555	-0.55469	-0.01765	0.142933	58.3795	0.679222
58.0616	109.639	38.8102	53.4444	26.8535	104	167.662	113.331	-0.55469	-0.01761	0.142933	58.5439	0.679211
59.1481	81.7925	32.1624	54.4132	26.8182	121.761	-134.979	80.4278	-0.55469	-0.01757	0.142933	58.7085	0.6792
60.0907	54.4033	50.036	55.2577	27.3619	141.679	-91.4587	47.8163	-0.55469	-0.01753	0.142933	58.8731	0.67919
60.6456	32.8219	76.6275	55.7784	28.2923	178.981	-69.3914	15.3878	-0.55469	-0.01749	0.142933	59.0379	0.679179
60.6921	33.5012	104.775	55.8782	29.309	-118.694	-52.1766	-17.0055	-0.55469	-0.01745	0.142933	59.2027	0.679168
60.2664	55.6826	131.333	55.5853	30.0894	-82.8575	-29.7541	-49.5143	-0.55469	-0.01741	0.142933	59.3677	0.679158
59.5523	83.337	148.677	55.0469	30.3766	-63.5609	15.3721	-82.2651	-0.55469	-0.01737	0.142933	59.5328	0.679147
58.8283	111.466	140.661	54.4934	30.0584	-46.1799	72.4905	-115.322	-0.5547	-0.01733	0.142933	59.6979	0.679136
57.6545	135.833	116.509	53.5485	29.6713	-19.638	101.258	-148.109	-0.55261	-0.02019	0.149007	59.2343	0.891356
57.6677	147.632	88.6372	53.6145	28.4813	31.4952	119.344	178.387	-0.55262	-0.02015	0.149007	59.3992	0.891347
58.2455	134.111	60.7637	54.1653	27.3901	80.5197	137.659	144.943	-0.55262	-0.02011	0.149007	59.5641	0.891338
59.2497	108.567	37.0373	55.0796	26.7479	105.221	168.789	111.746	-0.55262	-0.02007	0.149007	59.7292	0.891328
60.4044	80.3455	31.4379	56.1176	26.7404	122.285	-131.557	78.8797	-0.55262	-0.02003	0.149007	59.8944	0.891319
61.3928	52.6662	50.5957	57.0102	27.3413	141.922	-89.2773	46.3075	-0.55262	-0.01999	0.149007	60.0597	0.89131
61.9574	31.0524	77.7455	57.5445	28.3411	-179.448	-68.3027	13.9154	-0.55262	-0.01995	0.149007	60.2251	0.891301
61.9751	33.1352	106.22	57.6202	29.4195	-115.208	-51.6729	-18.4474	-0.55262	-0.01991	0.149007	60.3905	0.891292
61.4912	56.3709	133.021	57.2726	30.2358	-80.9424	-29.309	-50.9325	-0.55263	-0.01987	0.149007	60.5561	0.891283
60.7072	84.4797	150.09	56.6655	30.5224	-62.5857	17.7424	-83.6672	-0.55263	-0.01983	0.149007	60.7218	0.891274
59.9239	112.895	140.622	56.0514	30.1666	-45.6772	75.2889	-116.716	-0.55263	-0.01979	0.149007	60.8875	0.891265
59.4496	138.257	115.469	55.6975	29.2614	-19.328	102.934	-150.044	-0.55263	-0.01974	0.149007	61.0533	0.891256
59.0501	148.873	87.0018	55.4053	27.838	34.6135	119.638	176.503	-0.55142	-0.01779	0.154028	60.6989	1.01888
59.6678	133.662	58.8031	55.9959	26.8357	82.8904	137.587	143.121	-0.55143	-0.01775	0.154028	60.8651	1.01887
60.6718	107.329	34.9785	56.9196	26.2868	106.191	169.705	109.978	-0.55143	-0.01771	0.154028	61.0314	1.01887
61.788	78.6865	30.7854	57.9357	26.3478	122.509	-127.869	77.1368	-0.55143	-0.01767	0.154028	61.1979	1.01887
62.713	50.7088	51.4248	58.784	26.974	141.94	-87.3209	44.5568	-0.55143	-0.01763	0.154028	61.3645	1.01886
63.2094	29.2216	79.191	59.2657	27.9512	-177.538	-67.5809	12.1275	-0.55143	-0.01759	0.154028	61.5311	1.01886
63.1751	33.1742	108.027	59.2963	28.967	-111.704	-51.5605	-20.2911	-0.55143	-0.01755	0.154028	61.6978	1.01885
62.6721	57.5424	135.07	58.9254	29.6995	-79.4887	-29.1009	-52.8362	-0.55143	-0.01751	0.154028	61.8646	1.01885
61.9093	86.1366	151.597	58.3257	29.9064	-62.1592	20.6668	-85.6198	-0.55143	-0.01747	0.154028	62.0315	1.01884
61.1823	114.875	140.227	57.7498	29.5024	-45.7193	78.1304	-118.691	-0.55144	-0.01743	0.154028	62.1984	1.01884

Table A4. Sample 10 Hz File for AC6-A on 13 August 2015

year	month	day	hour	minute	second	alt	lat	lon	dos1l	dos1m	dos1rate	dos2l
2015	8	13	0	15	2	676.443	54.0555	139.881	62	78	-1.00E+31	42
2015	8	13	0	15	2.1	676.45	54.0614	139.879	63	78	10.0001	42
2015	8	13	0	15	2.2	676.457	54.0673	139.877	64	78	9.99905	42
2015	8	13	0	15	2.3	676.464	54.0733	139.874	65	78	10.0001	42
2015	8	13	0	15	2.4	676.471	54.0792	139.872	65	78	0	42
2015	8	13	0	15	2.5	676.479	54.0851	139.869	66	78	10.0001	42
2015	8	13	0	15	2.6	676.486	54.091	139.867	67	78	10.0001	42
2015	8	13	0	15	2.7	676.493	54.097	139.864	68	78	10.0001	42
2015	8	13	0	15	2.8	676.501	54.1029	139.862	68	78	0	42
2015	8	13	0	15	2.9	676.508	54.1088	139.859	69	78	10.0001	42
2015	8	13	0	15	3	676.516	54.1148	139.853	70	78	10.0001	42
2015	8	13	0	15	3.1	676.524	54.1207	139.85	71	78	10.0001	42
2015	8	13	0	15	3.2	676.532	54.1266	139.848	71	78	0	42
2015	8	13	0	15	3.3	676.539	54.1325	139.845	72	78	10.0001	42
2015	8	13	0	15	3.4	676.547	54.1385	139.843	73	78	10.0001	42
2015	8	13	0	15	3.5	676.555	54.1444	139.84	73	78	0	42
2015	8	13	0	15	3.6	676.564	54.1503	139.838	74	78	10.0001	42
2015	8	13	0	15	3.7	676.572	54.1563	139.835	75	78	10.0001	42
2015	8	13	0	15	3.8	676.58	54.1622	139.833	76	78	10.0001	42
2015	8	13	0	15	3.9	676.588	54.1681	139.83	76	78	0	42
2015	8	13	0	15	4	676.597	54.174	139.824	77	78	10.0001	42
2015	8	13	0	15	4.1	676.605	54.18	139.821	78	78	9.99905	42
2015	8	13	0	15	4.2	676.614	54.1859	139.819	79	78	10.0001	42
2015	8	13	0	15	4.3	676.623	54.1918	139.816	79	78	0	42
2015	8	13	0	15	4.4	676.632	54.1978	139.814	79	78	0	42
2015	8	13	0	15	4.5	676.64	54.2037	139.811	80	78	10.0001	42
2015	8	13	0	15	4.6	676.649	54.2096	139.809	81	78	10.0001	42
2015	8	13	0	15	4.7	676.658	54.2155	139.807	82	78	10.0001	42
2015	8	13	0	15	4.8	676.667	54.2215	139.804	82	78	0	42
2015	8	13	0	15	4.9	676.677	54.2274	139.802	83	78	10.0001	42
2015	8	13	0	15	5	676.686	54.2333	139.795	84	78	10.0001	42
2015	8	13	0	15	5.1	676.687	54.2393	139.792	84	78	0	42
2015	8	13	0	15	5.2	676.689	54.2452	139.79	84	78	0	42

dos2m	dos2rate	dos3l	dos3m	dos3rate	flag	Subcom	Lm_OPQ	Bmag_OPQ	MLT_OPQ	InvLat_OPQ	Loss_Cone_	K_Z
211	-1.00E+31	189	66	-1.00E+31	2	0	2.37439	40686.5	9.25536	49.5361	-1	-1.00E+31
211	0	188	66	0	2	1	2.37439	40686.5	9.25536	49.5361	-1	-1.00E+31
211	0	188	66	0	2	2	2.37439	40686.5	9.25536	49.5361	-1	-1.00E+31
211	0	188	66	0	2	3	2.37728	40696.1	9.25432	49.5657	-1	-1.00E+31
211	0	188	66	0	2	4	2.37728	40696.1	9.25432	49.5657	-1	-1.00E+31
211	0	188	66	0	2	5	2.37728	40696.1	9.25432	49.5657	-1	-1.00E+31
211	0	188	66	0	2	6	2.37728	40696.1	9.25432	49.5657	-1	-1.00E+31
211	0	188	66	0	2	7	2.37728	40696.1	9.25432	49.5657	-1	-1.00E+31
211	0	188	66	0	2	8	2.37728	40696.1	9.25432	49.5657	-1	-1.00E+31
211	0	188	66	0	2	9	2.37728	40696.1	9.25432	49.5657	-1	-1.00E+31
211	0	188	66	0	2	0	2.38372	40715.6	9.25226	49.6318	-1	-1.00E+31
211	0	188	66	0	2	1	2.38372	40715.6	9.25226	49.6318	-1	-1.00E+31
211	0	188	66	0	2	2	2.38372	40715.6	9.25226	49.6318	-1	-1.00E+31
211	0	188	66	0	2	3	2.38372	40715.6	9.25226	49.6318	-1	-1.00E+31
211	0	188	66	0	2	4	2.38372	40715.6	9.25226	49.6318	-1	-1.00E+31
211	0	188	66	0	2	5	2.38372	40715.6	9.25226	49.6318	-1	-1.00E+31
211	0	188	66	0	2	6	2.38372	40715.6	9.25226	49.6318	-1	-1.00E+31
211	0	188	66	0	2	7	2.38372	40715.6	9.25226	49.6318	-1	-1.00E+31
211	0	188	66	0	2	8	2.38372	40715.6	9.25226	49.6318	-1	-1.00E+31
211	0	188	66	0	2	9	2.38372	40715.6	9.25226	49.6318	-1	-1.00E+31
211	0	188	66	0	2	0	2.38372	40715.6	9.25226	49.6318	-1	-1.00E+31
211	0	188	66	0	2	1	2.39044	40736.7	9.24998	49.7002	-1	-1.00E+31
211	0	188	66	0	2	2	2.39044	40736.7	9.24998	49.7002	-1	-1.00E+31
211	0	188	66	0	2	3	2.39044	40736.7	9.24998	49.7002	-1	-1.00E+31
211	0	188	66	0	2	4	2.39044	40736.7	9.24998	49.7002	-1	-1.00E+31
211	0	188	66	0	2	5	2.39044	40736.7	9.24998	49.7002	-1	-1.00E+31
211	0	188	66	0	2	6	2.39044	40736.7	9.24998	49.7002	-1	-1.00E+31
211	0	188	66	0	2	7	2.39044	40736.7	9.24998	49.7002	-1	-1.00E+31
211	0	188	66	0	2	8	2.39044	40736.7	9.24998	49.7002	-1	-1.00E+31
211	0	188	66	0	2	9	2.39044	40736.7	9.24998	49.7002	-1	-1.00E+31
211	0	188	66	0	2	0	2.39044	40736.7	9.24998	49.7002	-1	-1.00E+31
211	0	188	66	0	2	1	2.3958	40754.7	9.24813	49.7546	-1	-1.00E+31
211	0	188	66	0	2	2	2.3958	40754.7	9.24813	49.7546	-1	-1.00E+31

Lstar_Z	hmin_Z	Alpha	Beta	Dist_In_Tra	Lag_In_Tra	Dist_Cross_	Dist_Cross_	Dist_Total
-1.00E+31	-1.00E+31	144.541	116.836	36.8721	4.90709	-0.16856	0.324236	36.8995
-1.00E+31	-1.00E+31	144.505	116.872	36.8721	4.90709	-0.16859	0.324258	36.8995
-1.00E+31	-1.00E+31	144.469	116.905	36.8721	4.9071	-0.16861	0.32428	36.8995
-1.00E+31	-1.00E+31	144.402	116.993	36.872	4.9071	-0.16864	0.324302	36.8995
-1.00E+31	-1.00E+31	144.364	117.018	36.872	4.9071	-0.16867	0.324323	36.8994
-1.00E+31	-1.00E+31	144.324	117.039	36.872	4.9071	-0.1687	0.324345	36.8994
-1.00E+31	-1.00E+31	144.285	117.056	36.872	4.9071	-0.16872	0.324367	36.8994
-1.00E+31	-1.00E+31	144.244	117.07	36.872	4.9071	-0.16875	0.324389	36.8994
-1.00E+31	-1.00E+31	144.204	117.079	36.872	4.9071	-0.16878	0.324411	36.8993
-1.00E+31	-1.00E+31	144.163	117.084	36.872	4.9071	-0.16881	0.324433	36.8993
-1.00E+31	-1.00E+31	144.064	117.205	36.8719	4.9071	-0.16883	0.324454	36.8993
-1.00E+31	-1.00E+31	144.023	117.202	36.8719	4.9071	-0.16886	0.324476	36.8993
-1.00E+31	-1.00E+31	143.983	117.195	36.8719	4.9071	-0.16889	0.324498	36.8993
-1.00E+31	-1.00E+31	143.942	117.185	36.8719	4.9071	-0.16892	0.32452	36.8992
-1.00E+31	-1.00E+31	143.903	117.171	36.8719	4.90711	-0.16894	0.324542	36.8992
-1.00E+31	-1.00E+31	143.864	117.153	36.8719	4.90711	-0.16897	0.324564	36.8992
-1.00E+31	-1.00E+31	143.825	117.131	36.8718	4.90711	-0.169	0.324585	36.8992
-1.00E+31	-1.00E+31	143.788	117.106	36.8718	4.90711	-0.16902	0.324607	36.8991
-1.00E+31	-1.00E+31	143.751	117.077	36.8718	4.90711	-0.16905	0.324629	36.8991
-1.00E+31	-1.00E+31	143.715	117.044	36.8718	4.90711	-0.16908	0.324651	36.8991
-1.00E+31	-1.00E+31	143.684	117.019	36.8718	4.90711	-0.16911	0.324673	36.8991
-1.00E+31	-1.00E+31	143.583	117.098	36.8718	4.90711	-0.16913	0.324695	36.899
-1.00E+31	-1.00E+31	143.552	117.056	36.8718	4.90711	-0.16916	0.324716	36.899
-1.00E+31	-1.00E+31	143.522	117.011	36.8717	4.90711	-0.16919	0.324738	36.899
-1.00E+31	-1.00E+31	143.493	116.963	36.8717	4.90711	-0.16922	0.32476	36.899
-1.00E+31	-1.00E+31	143.466	116.913	36.8717	4.90711	-0.16924	0.324782	36.8989
-1.00E+31	-1.00E+31	143.441	116.861	36.8717	4.90712	-0.16927	0.324804	36.8989
-1.00E+31	-1.00E+31	143.418	116.806	36.8717	4.90712	-0.1693	0.324826	36.8989
-1.00E+31	-1.00E+31	143.396	116.749	36.8717	4.90712	-0.16933	0.324847	36.8989
-1.00E+31	-1.00E+31	143.377	116.69	36.8716	4.90712	-0.16935	0.324869	36.8988
-1.00E+31	-1.00E+31	143.363	116.641	36.8716	4.90712	-0.16938	0.324891	36.8988
-1.00E+31	-1.00E+31	143.292	116.672	36.8716	4.90712	-0.16941	0.324913	36.8988
-1.00E+31	-1.00E+31	143.279	116.609	36.8716	4.90712	-0.16943	0.324935	36.8988

External Distribution

REPORT TITLE

AeroCube-6 Dosimeter Data README (v3.0)

REPORT NO.	PUBLICATION DATE	SECURITY CLASSIFICATION
TOR-2016-01155	March 4, 2016	UNCLASSIFIED

Maria Scardera
SMC/ADXC
maria.scardera@us.af.mil

Col. Sean Rucker
SMC/AD
john.anttonen@us.af.mil

Troy Tschirhart
SMC/AD
troy.tschirhart.1@us.af.mil

Roberta Ewart
SMC/AD
roberta.ewart@us.af.mil

Jim Taniguchi
SMC/AD
james.taniguchi@us.af.mil

Lt. Col. Donny White
SMC/AD
donny.white@us.af.mil

Col. Jeff Stutz
SMC/AD
jeffrey.stutz@us.af.mil

Vince Caponpon
SMC/AD
vincent.caponpon@us.af.mil

Alex Levi
SMC/AD
alejandro.levi.1@us.af.mil

Col. Jim Planeaux
SMC/AD
james.planeaux@us.af.mil

Nabil Attallah
SMC/AD
nabil.attallah@us.af.mil

Lt. Col. Kendra Crider
SMC/ADYT
kendra.crider@us.af.mil

Col. John Anttonen
SMC/AD
john.anttonen@us.af.mil

Doug Brown
SMC/AD
douglas.brown.35@us.af.mil

Col. Jason Cothern
SMC/AD
donald.cothern@us.af.mil

Nhung Tran
SMC/ADSH
nhung.tran@us.af.mil

Jonwa Kim
SMC/ADSH
jonwa.kim.2@us.af.mil

Justin Shimasaki
SMC/ADSH
Justin.shimasaki.1@usaf.mil

APPROVED BY (AF OFFICE) NA DATE

AEROSPACE REPORT NO.
TOR-2016-01155

AeroCube-6 Dosimeter Data README (v3.0)

Approved Electronically by:

James L. Roeder,
DIRECTOR
SPACE SCIENCES
DEPARTMENT
SPACE SCIENCE
APPLICATIONS
LABORATORY
ENGINEERING &
TECHNOLOGY GROUP

James G. Gee, PRINC
DIRECTOR
DEVELOPMENTAL
PLANNING & PROJECTS
DEVELOPMENTAL
PLANNING &
ARCHITECTURES
SYSTEMS PLANNING
ENGINEERING & QUALITY

Rand H. Fisher, SR VP
SPEQ
SYSTEMS PLANNING
ENGINEERING & QUALITY

Technical Peer Review Performed by:

Catherine C. Venturini,
PROJECT LEADER
SPACE & GROUND
DEVELOPMENTAL
PLANNING & PROJECTS
SYSTEMS PLANNING
ENGINEERING & QUALITY

Drew L. Turner, MEMBER-
TECH STF
IONOSPHERIC &
ATMOSPHERIC SCIENCES
SPACE SCIENCES
DEPARTMENT
ENGINEERING &
TECHNOLOGY GROUP

SC2603